# The Calorimeter First Level Trigger Processor, & Studies after the Upgrade at the ZEUS Experiment at HERA

John Loizides

University College London/Argonne National Laboratory

$1^{st}$ Year Transfer Report*

June 14, 2002

**Abstract**

An explanation of the work carried out in the first twelve months of my postgraduate degree is presented. Work has been carried out on the Calorimeter First Level Trigger Processor (CFLTP) which has been the bulk of my activities. This is so the CFLTP is prepared for the new running period of the ZEUS experiment at HERA. The CFLTP is a complex system and will be explained in detail along with the role it plays in the Calorimeter First Level Trigger (CFLT) chain and Data Acquisition System (DAQ). A Charge Injection and Physics timing calibration has been carried out and resulted in ZEUS-Note-02-010.

A proposal for the first trigger using information from the Global Tracking Trigger (GTT) is discussed. The motivation for this is, to attain rough rate estimate reduction factor in the trigger considered and possible further developments are presented.

Lastly, a Monte Carlo Study of $B^0$ Meson Production in Zeus is detailed. A well understood decay chain is chosen to evaluate the problems for effective exploitation of the recently installed Micro Vertex Detector (MVD) some initial findings are shown. This is the beginning of the core work that will compose my thesis.

*Submitted for the transfer from M. Phil to Ph. D. Status

# Contents



# List of Figures

# List of Tables

# 1 Introduction

The Hadron Electron Ring Accelerator (HERA) is the only electron-proton collider in the world. HERA was constructed to study high energy scattering between electrons of 27.5 GeV and protons of 920 GeV. HERA is 6.3 $km$ in circumference and is approximately 10m-25m underground.

The Zeus multipurpose detector is designed to measure $e^{\pm}p$ interactions at HERA. The primary components used for every analysis are the compensating Uranium-Scintillator Calorimeter (CAL), the central tracking detector (CTD), and luminosity detector (LUMI).

The Zeus detector Fig. 1 and Hera have been undergoing a major upgrade for the past year and a half. There have been several major improvements to the experiment, the Micro-Vertex detector (MVD), the Global Tracking Trigger (GTT), and the Straw Tube Tracker (STT) which are some of these upgrades. The STT has replaced the Transition Radiation Detector (TRD) as a part of the Forward Detector (FDET) designed to measure the characteristics of forward going particles. The main goal of the MVD is the possibility to tag heavy quarks decaying from baryons or mesons very close to the nominal vertex position. Long lifetimes of the order of $10^{-12}$ $s$ for charm and beauty decays mean that they can be identified through displaced vertices in the MVD. These vertices will be of the order of 200 $\mu m$.

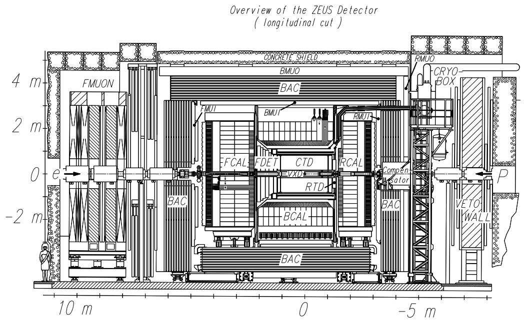


Figure 1: The Zeus Detector

# 2 The Calorimeter First Level Trigger and the Calorimeter Trigger Processor

The Calorimeter Fist Level Trigger (CFLT) and the Calorimeter Trigger Processor (CFLTP) sit in the first level of the Zeus Data Acquisition System (DAQ) Fig. 2.

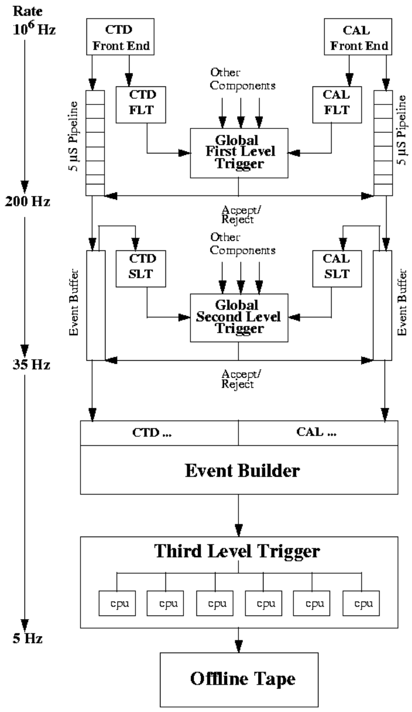


Figure 2: The Zeus Data Acquisition Chain

The First Level Trigger (FLT) has approximately $5\mu s$ or 52 bunch crossings to determine whether to keep the event or reject it, if it falls out of this time limit the event is lost. The FLT is completely pipelined, i.e. the whole process of the FLT is in hardware to reduce the amount of dead-time. The Global First Level trigger (GFLT) [1] receives the information from all of the local FLT's when the event is accepted and makes a more decisive decision based on the component information it received; it has $2.2\mu s$ after receiving the information from the local FLT's in which to make its decision.

The CFLT chain has the job of calculating the energy deposits and general information about the CAL, then passing it on to the FLT. The FLT has the task of reducing rate by getting rid of most of the beam gas and beam-halo background.

HERA's bunch crossing rate is every 96 $ns$ which corresponds to a rate of 10 $MHz$. The background rate is about 10 $kHz$, the rate is brought down to $10 - 200$ $kHz$ online with the amount of actual interesting $e^{\pm}p$ interactions being at about 5 $Hz$. As the input rates for each trigger stage decrease the complexity of algorithms and time each stage has to perform then increases; Zeus has adopted a three level trigger system.

## 2.1 CFLT

The CAL geometry plays a big part in the design of the CFLT. The Forward Calorimeter (FCAL) and Rear Calorimeter (RCAL) have modules running vertically. The modules run longitudinally in the case of the Barrel Calorimeter (BCAL). The modules are separated into towers shown in Fig. 3.

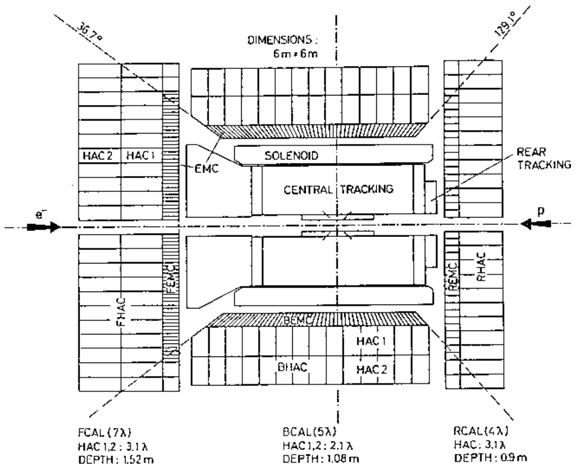


Figure 3: The Zeus Calorimeter

The first interaction length is made up of Electromagnetic Cells (EMC) then there are Hadronic Cells (HAC), two in the BCAL and FCAL and only one in the RCAL, due to the asymmetry in the beams. Most of the energies are typically deposited in the barrel or forward regions, with the deep inelastically scattered electron in the RCAL.

These data are stored in a pipeline clock clocked at 96 $ns$ for 5 $\mu s$ while the first level trigger concludes its decision about the event. The CFLT operates on a subset of the full data. In order to keep up with the incoming data the CFLT digitizes PhotoMultiplier Tube (PMT) pulses, to reduce the amount of electronics, cables, and crate backplane required; these data are at several points multiplexed in time before being sent to the CFLTP.

Figure 4 shows the organization of the CFLT. I will not go into great detail but more can be found at[2, 3]. The non-projectiveness of the front and rear calorimeter provides complications in order to

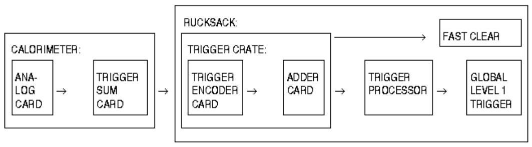


Figure 4: Data Flow in the CLFT Chain

be able to identify electrons or pions.

Figure 5 shows how the energy would be deposited in the CAL if the CAL was projective or non-projective. It is clear to see that the total energy deposited would overlap in a non-projective CAL but would be neatly within one tower/module in a projective CAL.

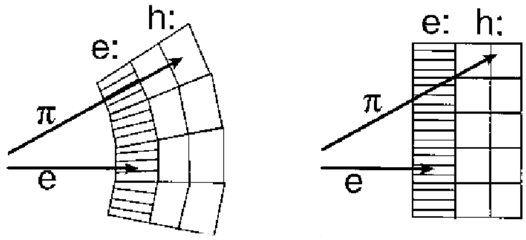


Figure 5: Projective Calorimeter, Non-Projective Calorimeter (left and right respectively)

The Calorimeter is divided into 16 regions the CFLT map their 16 crates to each region. The trick of tower arranging is done to compensate for the overlap in these energies not being contained within each tower/module. This arrangement can be seen in Fig. 6. The $e^{\pm}p$ collision at the nominal interaction point shows that the particles will deposit themselves in various modules so to reconstruct the correct energies in the CAL the modules have been positioned to accomodate these affects in order to do pattern recognition and energy summing correctly.

Then mapping of all the correct towers allows for quantities such as number of isolated electron and energies in towers as well as many other quantities to be calculated. Fig. 7 shows how isolated electrons are identified by the CFLT. There are three stages in the calculation. Firstly the pattern known as the "Micky Mouse" pattern is tried. The goal is to eliminate regions which could show energy that effect the decision therefore ruling out the possibility of an isolated electron. This is done onboard the Adder Cards which know about the X and Y regions of the region in which they are in, but do not know anything else about any other Adder Card. The CFLTP receives its information from all Adder Cards and bridges the gap between all Adder Cards, being able to see all regions allows the final definitive decision to be made.

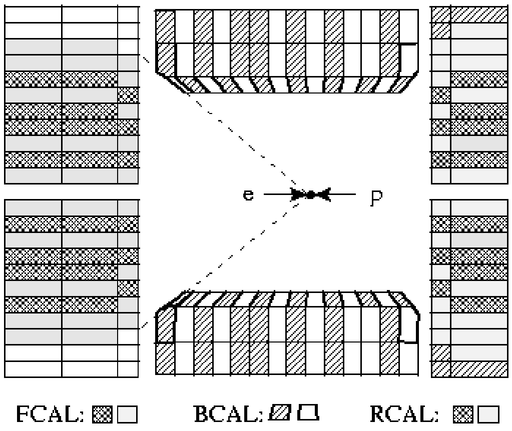


Figure 6: *ep* collision Tower Mapping in the Calorimeter

If there were to be an electron on the edge of one region, the Adder Card would not be able to make a decision on whether that electron was isolated or not because it would not have all the information it needs. The CFLTP then will do a similar pattern recognition in its Algorithm cards to match up the edges of all regions and see which ones are quiet or hold energy.

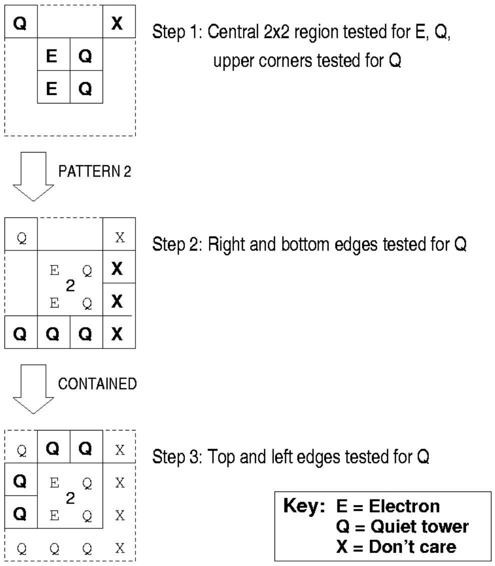


Figure 7: Isolated Electron Identification

## 2.2 The CFLTP

The CFLTP, Fig. 8 is at the heart of the final operations in the CFLT chain. Physically, it can be found on the third floor of the rucksack in the Zeus hall in the middle of the CFLT crates. It is made up of eight Input Cards, eight Algorithm Cards, four Output Cards, an os9 computer and a Communications Card (Comm Card). All sixteen regions of the CFLT send data to the CFLTP. It calculates Total Energy, Transverse Energy, number of isolated electrons, number of isolated muons and threshold information for the entire detector. It then send the compiled information to the GFLT for a decision to be made. The total amount of time the CFLTP has in order to complete its decision is less then 2.2 $\mu s$. The Algorithm cards give flexibility to the system, they are basically lookup tables which compute these data sent to them. They are hardwired so that the computation of the quantity that is required is delivered quickly. Algorithm cards are downloaded with tables that do this summing and other quantity calculations. This gives functionality, because they can be asked to miss out certain values or change the way the summation is done without swapping any hardware.

These data received by the CFLTP from the CFLT pass through the CFLTP system in a complicated way [5]. The CFLT has multiplexed these data in time, so the CFLTP has to be demultiplexed internally so that the calculations can be made. Four Quantities travel on each cable in 96 $ns$ steps, so these data are demultiplexed these and latched into the memories of the Input Cards. An exercise was performed by my Argonne Colleagues and I to make sure that the phase of the CFLTP and CFLT backplane were in sync with each other. This means that we were correctly latching the data sent to us and processing it correctly. In some cases this is not trivial as both Energy and Transverse Energy travel 24 $ns$ out of phase with each other on the same cable and could easily be mixed up, it is a little more complicated then this but simply the difficulty can be seen. This exercise was done by looking at certain quantities and understanding that the output made "physics sense" using the Adder test Program[4]. The reason for doing this was that for the year 2002 running of Zeus the CFLTP has been equipped with a New Comm Card. The function of this Comm Card is central to the system. It has the job of controlling all clocks of the system and control signals, as well as simulating the GFLT internally for tests. The commissioning of this Comm Card has now been completed.

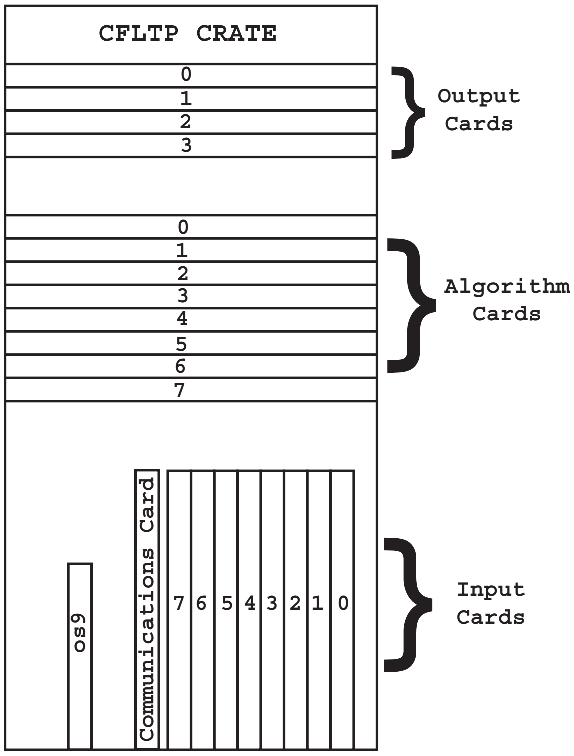


Figure 8: The CFLTP Crate Layout

### 2.2.1 CFLTP Work Carried Out

These past few months the CFLTP has gone through a number of various test which I have worked on with Antonio Pellegrino and Danny Krakauer (My colleagues from Argonne).

In February we used the CFLT Jade test facility located in the Jade hall at the Deutsches Elektronen-Synchrotron (DESY), to debug and fix two Input Cards. This must be read knowing that for a long period of time there has only ever been one spare Input Card. For this we also had to test them in the Zeus Hall. We only used two slots (slots 0 and 1) out of the eight for these tests because of the amount of cables which would have needed to be removed and the difficulties in doing this could have resulted in other problems. We successfully saw all the spares in the system work. We have various methods of doing these tests but they are too technical to cover in this report. One should understand that the Input cards are the most fragile of the system and have failed the most out of any component in the CFLTP system.

Part of understanding how the CFLTP works is to run a series of digital tests through the system and make sure there are no anomilises pointing to stuck bits or other faults. Tests concluded in March that the system started to behave in strange ways a while after we had been testing the system. I noticed that we were registering deposits in the CAL even though we had no beam! Consistently internal tests on the system isolated this down to a few bits on one Input Card which seemed to be always stuck high. This corresponded to a rate of 10 $M$Hz in some slots at the FLT, i.e. on every bunch crossing. Unfortunately these slots that were overflowing happened to be some of the most important slots, as the overflowing quantities were global energy quantities. So the situation was such that Zeus could not take any meaningful physics data. Therefore the pressure to get this working was quite intense as HERA was imminent in delivering luminosity.

Within the system we have the algorithm cards which can be programmed to sum energies and calculate certain quantities as described earlier. Therefore in the short term a solution to mask out the bits that were being affected until we could risk pulling the card out and finding the fault that way was devised. This was because the cards are too fragile to be constantly pulled out until the complete diagnosis is done without touching them.

With my colleagues from Argonne I learned how to prepare a new versions of the algorithm tables which are downloaded onto the algorithm cards. This then gave the result that these bits were masked but the CFLTP was then less efficient, because if energy was deposited in the CAL corresponding to those masked values we would not see them.

What happend was that there were quantities changing that were not previously causing rate problems, such as number of isolated electrons and FCAL energy. This meant that the digital problems within the CFLT or CFLTP were changing. There were several methods and tools used to see at which place the problem had occurred. The CFLTP sends these data through three places internally on its backplane where these data could be getting corrupted. These data are sent through the Input Cards via the backplane to the Algorithm Cards then the output is sent to the Output Cards again via the backplane. All these are places where the problems could have been occurring, starting in the Input Cards when these data are being latched, in the Algorithm Cards, passing through the backplane not being sent to the Output Cards properly. All these possibilities were checked meticulously.

The situation became very serious as the all possible software tests and diagnosises had been performed and there seemed to be no solution other then to start pulling out cards in the system. What was done was to touch every single pin on the back of the CFLTP backplane Fig. 9 with an oscilloscope probe using a special command internal to the CFLTP which toggles every single pin on the backplane. There are two regions of the CFLT on each input card with 128 *pins* per region to be checked. From this test we would see clearly if the Input Card affected was sending any data through so the algorithm cards could perform there procedures and results for the Output Cards.

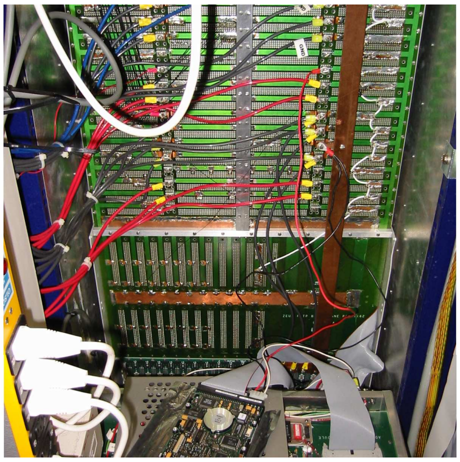

Figure 9: The CFLTP Backplane

What was found was that there were pins that were not reporting changes in voltages they were either stuck high or low on one Input Card. This then meant we either had a broken pin on the backplane or there was a continuity problem or the card (Slot 0) was not sitting properly. The fix was then to pull out the card and and another one next to it in order to get some leverage to force the other card in harder, after checking that there was no damage done to the backplane. This was a risky situation to be in because these cards are at an age when they have been pulled in and out of the system many times and are very fragile. The card was successfully inserted again as was the one next to it, and the system resumed to function in its normal way.

The final commissioning that needed to be done was to perform timing tests and map out and set the correct bunch crossing number offsets for the New Comm Card, and set the correct clock to match the phase of the CFLT clock with that of the CFLTP backplane's.

After this was done the CFLTP Comm Card had been successfully integrated with the CFLT, CAL DAQ and GFLT systems. As of April 19*th* 2002 the CFLTP was ready for luminosity running.

## 2.3 Calorimeter First Level Trigger Charge Injection Timing Calibration

Both the CFLT and CAL rely on Charge Injection ($Q_{inj}$) test pulses to perform a gain and timing calibration. This is so that each individual channel can have it's delay set to the optimum position, tuning each channel towards the "real physics" timing. There is a factor effecting this which is the timing window in which the CFLT can be calibrated. This is because the CFLT hardware requires some rise time to be sure to be latching (i.e. storing data in memory) correctly, then some time until the next data arrives in the front end cards for the front end cards to settle down. This timing window is approximately 40 $ns$.

I have co-written a Zeus Note [7] describing the way the way the calibration the CFLT and CAL was done in such a way as to make the CFLT as efficient as possible. Figure 10 shows the complex timing setup and how by changing one delay can affect the timing calibration of the other system.

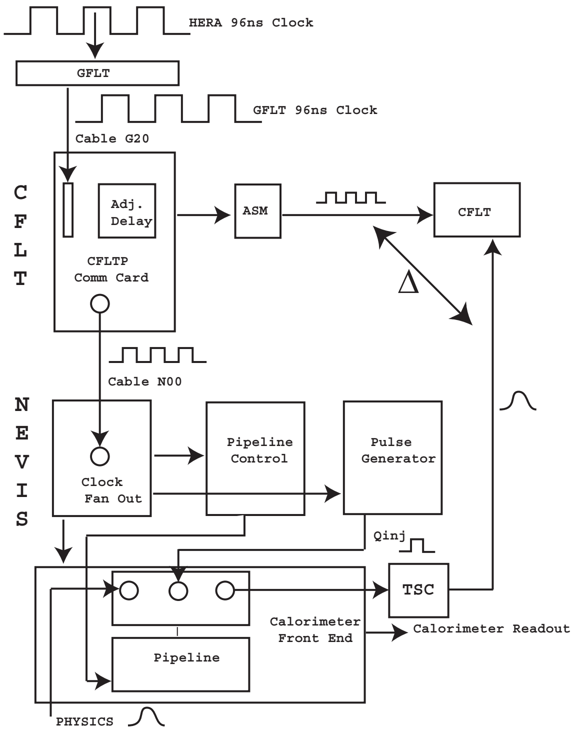


Figure 10: Timing diagram overview of CFLT and CAL

The Zeus note explains in more detail about how this calibration was done as well as some of the subtleties which must be taken into account whilst doing this calibration.

The conclusion of this exercise was that of calibrating both the CAL and CFLT to be in optimum efficiency and therefore fixing ($\Delta$). It is then the case by changing cable G20 from the GFLT to the Comm Card we could shift the CAL pipeline clock towards "physics" centering it about zero, but not changing the relative delay ($\Delta$) between the CAL and CFLT. In the past cable N00 has been the one which has been lengthend/shortend to do this calibration for the CAL, directly affecting the CFLT. This has been not noticed because of the GFLT not changing its timing significantly and always trying to compensate for shifts in HERA timing. In the new run HERA has changed it's clock by approximately 6 $ns$ and Zeus has completely new timing hardware which the GFLT bases itself on e.g. a new C5, meaning that these calibrations looked strange and after much investigation we narrowed it down to this reason. Figures 24 and 25 show a result of a proton run un-calibrated then a proton run after the re-calibration was performed.

# 3 Motivational Micro Vertex Trigger Study

The FLT triggers are based mainly on global and regional energy sums, quick calculations to see if there are any tracks pointing to the nominal vertex position and information from a few other components. Varieties of these quantities are required to fire FLT slots, which are designed to allow a certain type of event to be triggered on. These rough algorithms bring down the rate to about 300 $Hz$ from typical year 2000 running. The slots definitions are in fact a words which correspond to bits turned off or on.

Due to the new running period there have been many modifications to these slots to reduce the rate due to the new high luminosity running otherwise we would be swamped with rate and not be able to cope at the FLT. The dijet trigger chain used for many Zeus publications at HERA I which was well understood is one which has been modified due to the high rate. FLT slot 42 has been prescaled to zero for the new running phase, this has been in the past a well understood trigger. The New trigger chain replacement that has been put forward which contains an "or" of 17 FLT slots instead. This is unreasonably complicated, and difficult to simulate offline. What was looked at was to keep the grounding of the old trigger configuration with the replacement for slot 42 which is now slot 50 (definitions in Table 1), and adding a new $Z_{vertex}$ cut in the Second Level Trigger (SLT) Global tracking trigger (GTT) to reduce the rate. Also to motivate the slot to be used when new data arrives to understand the efficiency of the slot and help understand how well the GTT is working in CTD mode only. Then for a later study expand the slot to the Third Level Trigger (TLT) and get a bit more adventurous and include MVD information to do some secondary impact parameters, once the MVD information can be trusted as well as adding MVD information to the SLT trigger.

| Quantity | SLOT 42 | SLOT 50 |
|---|---|---|
| CAL_E | > 14.968 GeV | > 14.968 GeV |
| EMC_E | > 10.068 GeV | > 10.068 GeV |
| BEMC_E | > 3.4040 GeV | > 3.4040 GeV |
| REMC_E | > 2.0320 GeV | > 2.0320 GeV |
| TRK_q95b | > 3.4040 GeV | > 3.4040 GeV |
| CAL_Et | NO CUT | > 7.0000 GeV |

Table 1: FLT SLOT 42 and SLOT 50 Definitions

To evaluate the rate reduction of these changes on the trigger rate, a sample SLT passthroughs were used. A passthrough event means that the event is allowed to go through the DAQ chain only after being selected by the FLT bits, but with no SLT and TLT selection. This then allows an analysis to be done to see how beam gas events, shown in Fig. 11 contribute and how the rates of these slots behave. SLT and TLT rates can be studied and triggers can be designed given this information. The assumption is that the relative rate reduction found from 2000 data will be approximate that in the upgrade data. Only studies later with real data will confirm the true values for the rate reduction.

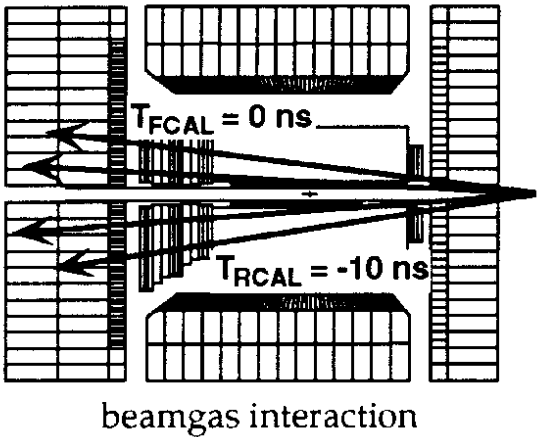


Figure 11: Beam-Gas Interaction, RCAL(background) right, FCAL left

Figure 12 shows how the GTT reconstructs the $Z$ vertex's of this passthrough sample which contains a mixture of beam gas interactions as well as *ep* collisions. The beam gas interactions are characterized by the underlying distribution peaking in the negative $Z$ direction due to the interactions of the proton in the beam pipe with beam gas. The central peak is around the nominal interaction point $(1.75, 0, 0)$ *cm* of the Zeus coordinate system[1] (x, y, z) respectively which is the new nominal interaction region for positrons. For electrons the nominal position will be $(1.0, 0, 0)$ *cm*.

To understand what kind of effect any extra cut placed on the $Z$ vertex distribution would have on the sample the resolution of the GTT in CTD-ONLY mode was studied. Figure 13 shows the result of a two Gaussian fit to the $Z_{fmckin}$ - $Z_{gtt}$. Where $Z_{fmckin}$ corresponds to the true vertex information and $Z_{gtt}$ information is that which is found by the GTT algorithm. There is also is a comparison with the TLT reconstruction. These were both fitted with two Gaussian's because of the way the GTT algorithm works. The GTT has no information about the z−by−timing hits in the CTD, but uses the stereo layers instead to

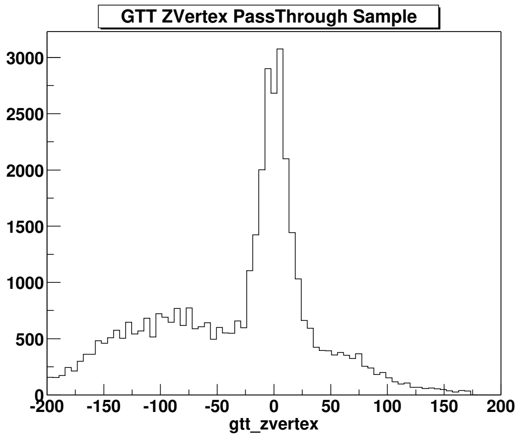


Figure 12: $Z$ vertex (cm) of the passthrough sample as reconstructed by the Global Tracking Trigger, running in CTD-ONLY mode

reconstruct the tracks. This leads to inefficiencies in the algorithm that cannot be got around because of the coverage of the CTD. When you are at low angles in the CTD only a few of the stereo layers are contributing to the track reconstruction. This leads to the non Gaussian tails in the fit which is why the two Gaussian are fitted to the plots. The results of my fits shown in Fig. 13 are comparable to those given in [10, 11] indicating consistency.

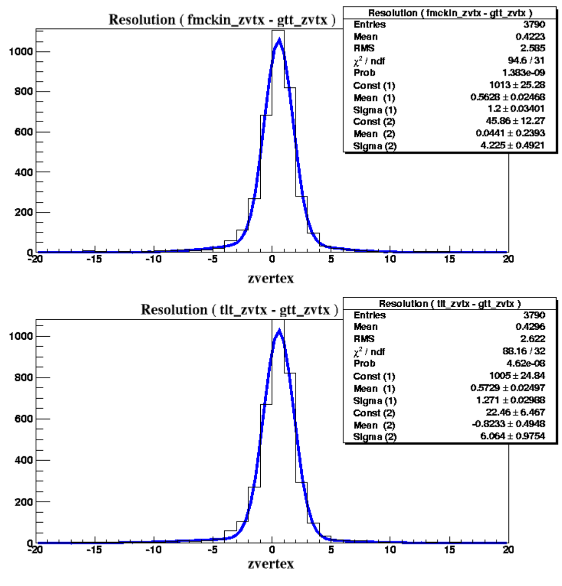


Figure 13: The top plot shows resolution ($Z_{fmckin}$ - $Z_{gtt}$) in (cm). The Bottom plot shows resolution ($Z_{tlt}$ - $Z_{gtt}$) in (cm)

The result shown in fig. 13 allow the cut to be placed with an uncertainly of $\pm$ 1 *cm*. The effect of this as a systematic error upon an analysis is expected to be small. Figure 14 shows the distribution of the vertices fired by HFL SLOT 1 in the passthrough sample. HFL SLOT 1 is the

[1]The ZEUS coordinate system is a right-handed Cartesian system, with the $Z$ axis pointing in the proton beam direction, referred to as the "forward direction", and the $X$ axis pointing left towards the center of HERA. The coordinate origin is at the nominal interaction point.

SLT trigger slot under study.

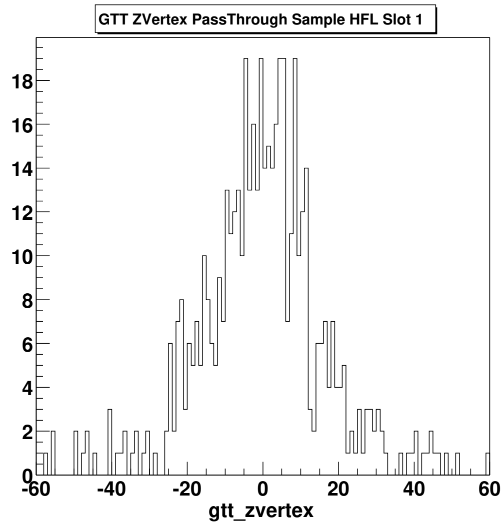


Figure 14: $Z$ vertices in the sample that fired HFL SLOT 1

The New Proposal for HFL1 suggested is: (changes over the persently marked scheme are highlighted in bold)

- FLT SLOT 40/41/**50**/43
- $-60\ cm\ <\ Z_{CTD-SLTvertex}\ <\ 60\ cm$
- $E\ -\ Pz\ > 2\ Gev$
- $ET\ > 12$
- $pz/E\ <\ 0.96$
- $\mathbf{-20\ cm\ <\ Z_{GTTVERTEX}\ < 20\ cm}$

Figure 15 shows how by placing an additional $Z$ vertex cut found by the GTT of plus minus the $Z$ vertex in centimeters along the abscissa affects the acceptance of the events in that slot. A passthrough sample was used which had the vertex distribution shown in Fig. 12. The minimum bias $ep$ collision distributed vertex was used which was taken from the 1998/1999 run [8]. The postupgrade $ep$ vertex distribution is expected to be similar.

Two Monte Carlo curves were added to see how a pure sample of heavy quarks is affected by this slot. Both Monte Carlo curves are pure samples of $D^*$ mesons fired by the old HF1 dijet trigger chain. This is to check against the old dijet trigger which is well understood in terms of efficiency, and give an understanding about the proposed trigger slot.

What can be seen from the rate reduction at $|Z|\ < 20$ will be greater for passthroughs then for "physics" indicating that at $|Z|\ < 20$ physics would be cut by 10 % and passthroughs by 20 %

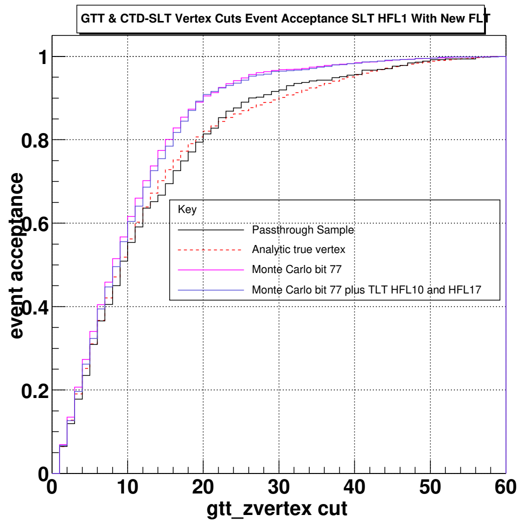


Figure 15: GTT Z vertex (cm) cut of plus minus of the value of the x axis. The y-axis indicates the event acceptance for any given value of the cut

by this cut on the vertex. However, the MVD is approximately between $|Z|\ < 20$ therefore it is better to have a sample dominated by events near the nominal vertex which give a good MVD acceptance. The combined rate reduction for this proposed slot would be of the order of 40 % less then that of the currently implemented HFL1. This trigger also does not take mutually exclusive events, so this would allow the niche in which the MVD triggers could be based on so that once data is being understood the events with impact parameters which could be reconstructed by the MVD would have to be within this extra GTT $Z$ vertex cut only because of the acceptance region of the MVD. This would allow for pattern recognition and anlysis of impact parameters.

# 4 Background Studies at HERA

During the recommisioning phase after the upgrade HERA has been experiencing a number of problems with tuning for Zeus and H1 (the second large experiment at DESY). The background levels which are composed of proton beam-gas Fig. 11 and synchrotron radiation from the positron beam have been looked at.

The beam-gas contribution is significantly bad due to the vacuum within the beampipe not being as good as it should be. The vacuum should be of the order $10^{-9}$ *bar* which is acceptable with high currents, but $10^{-10} - 10^{-11}$ *bar* should be the normal state. The current status is that it has been as bad as $10^{-6}$ *bar* and at present is an order of magnitude worse then it should be in the long term and improving slowly. The beampipe needs a procedure referred to as "backing out" the vacuum. Baking out the vacuum is essentially putting very high positron current beams into the HERA ring and heating it up in order to extract the gas in the walls of the beampipe out, which can then be pumped out, improving the conditions. This is a lengthy procedure, the estimated amount of current needed in order for a good vacuum to be attained is 30 *Amp hours*, and is being done parasiticly with commissioning luminosity.

As a product of my monitoring of the CFLTP, I have been able to contribute towards the understanding of the background issues in Zeus.

After looking at timing plots of the calorimeter I was able to identify another background contribution, which was the proton beam hitting a collimator. Prior to this it had been assumed that all the proton background problems came from the high rate of proton beam-gas interactions. It can be seen clearly in Fig. 16 that there is double peaked structure in RCAL timing.

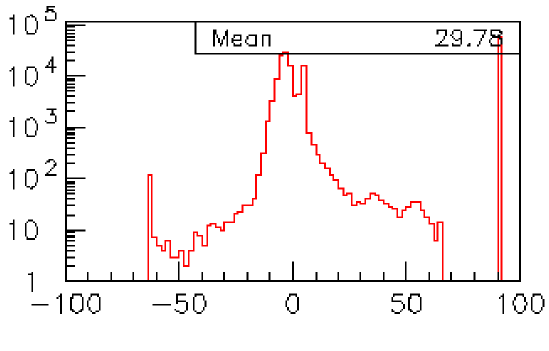


Figure 16: RCAL Timing CAL Timing plot from the online Golbal Second Level Trigger histogram presenter

$T = 0$ *ns* is calibrated in such a way as the "physics" coming from the noiminal interaction region is centered around 0 a reference marker. The first peak that is at around $-5$ *ns* corresponds to 80 *cm* in $Z$ from the RCAL which is the position where a collimator positioned.

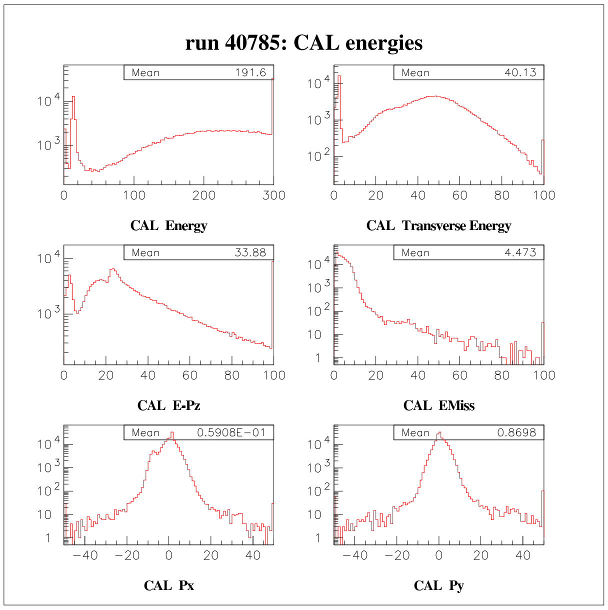


Figure 17: CAL Energy plots from the online GSLT histogram presenter

There is also an uncharacteristic bulge in the $Px$ distribution of the CAL energy. This shows that there is some kind of deposit in the negative $x$ direction which is another problem related to the positron beam.

My findings have been confirmed by others looking at various other distributions and can be understood by in the case of off momentum protons getting bent by the last bending magnet (GG) sweeping them into the collimator and creating hits into the RCAL. The timing peak is shifted to the left by $-5$ *ns* because the protons hit the collimator before passing through the interaction region. The solutions to this problem are to get a better vacuum or to move the beam slightly so it doesn't hit the collimator. However there is the problem of the synchrotron radiation maybe not allowing this. All possiblities are being looked at.

# 5 Beauty Production at HERA II

A region of physics which will be able to be studied with far greater precision after the upgrade is heavy flavour physics. Procceses unique to HERA hopefully give an insight into why other experiments have seen a cross-section of $B$ mesons and baryons of two to three times as high as the current predictions. There are many models which try to describe these data, HERA provides this oportunity to measure the properties of these heavy quarks which are a direct probe of the gluon. The MVD will allow for a tagging heavy quarks and help to identify them from their decay and fragmentation products.

## 5.1 Monte Carlo Beauty study

### 5.1.1 Beauty in Deep Inelastic Scattering

A feasibility study was done looking for the number Beauty events that would be seen in Deep Inelastic Scattering (DIS) $Q^2 > 1$ GeV Fig. 18 in the most favorable channels according to the Monte Carlo program Aroma [15].

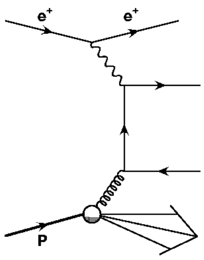


Figure 18: DIS Feynman Diagram at HERA

Table 2 shows the branching ratios of beauty mesons/baryons as the percentage of total beauty production in DIS found by Aroma.

| Beauty Meson/Baryon | Branching Ratio |
|---|---|
| $B^0$ | 23.5% |
| $B^+$ | 17.5% |
| $B^{*0}$ | 23.5% |
| $B^{*+}$ | 17.5% |
| $B_s^0$ | 7% |
| $B_s^{*0}$ | 5% |
| $\Lambda_b^0$ | 5% |

Table 2: DIS Channels Branching Ratio's greater than or equal to five percent in the Monte Carlo generator Aroma

The decay channels of these mesons were then looked at using only where the decay chain can be fully reconstructed were considered. The aim was to determine the possibility at looking at a particular beauty meson/baryon channel in DIS. By looking into the Particle Data Group (PDG) year 2000 values and the most probable channels were selected and studied to at how many events would be seen with a given cross section and luminosity generated. It was found that it would require the whole of the Zeus running until 2005 when HERA will have delivered a luminosity of $1fb^{-1}$ to have in the region of 1000 events without taking into account detector acceptance which is of the order 40%, then being able to fully reconstruct them which is of the order 10% for these particular channels in Table 3. The number of events that were generated in each case were 10000 giving a total cross-section of 517 $pb$, these were the largest Branching ratio channels in the PDG. Therefore this study showed that it would not be feasible to look at beauty production in DIS for an initial study but would be reasonable later in Zeus running time.

| Decay Channel | # of Events Found |
|---|---|
| $B^{\pm} \to J/\Psi\ K^{\pm}$ $J/\Psi \to e^+e^-$ | 6 |
| $B^{\pm} \to J/\Psi\ K^{\pm}$ $J/\Psi \to \mu^+\mu^-$ | 4 |
| $B^+ \to l^+V_l$ *anything* & $B^0 \to l^+V_l$ *anything* | 148 |

Table 3: DIS Channels Branching Ratio's greater than or equal to five percent according to PDG year 2002 values

### 5.1.2 Beauty in Photoproduction

An Electron/positron is surrounded by a cloud of virtual photons emitted by it. A gluon in the proton beam can collide with a virtual photon produced by an electron/positron and cause a photoproduction event. The electron/positron does not interact with the proton directly in a photoproduction event, it is not therefore scattered greatly and will probably escape down the beam-pipe hole without being detected. These events will have a low momentum transfer ($Q^2$). $Q^2 < 1$ is often the definition of photoproduction at HERA. Also these events will be azimutally symmetric, meaning that the missing transverse energy compared with the total transverse energy will be small.

The photoproduction cross sections dominate over the DIS cross sections therefore the heavy flavour production in photoproduction will have greater statistics. Pythia [12] was used to generate a sample of direct and resolved photoproduction

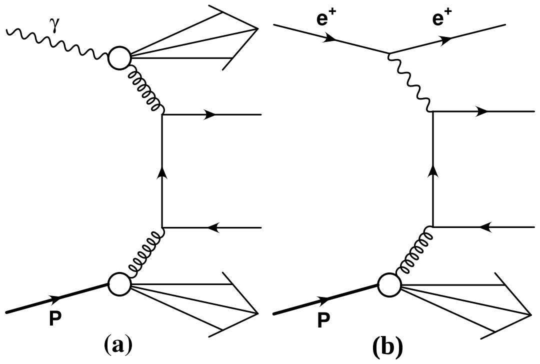


Figure 19: Leading order Feynman Diagrams Corresponding to Resolved Photoproduction (a) and Direct Photoproduction (b)

events Fig. 19.

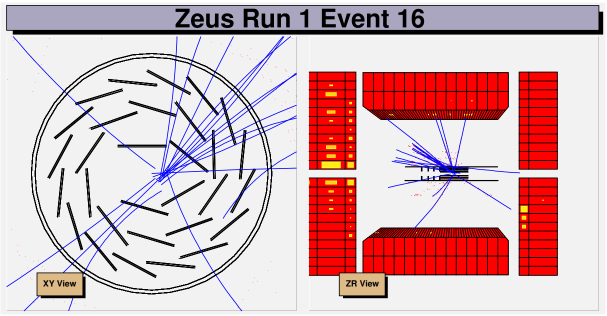


Figure 20: Direct Photoproduction event using the new event display, left shows the MVD, right the ZR view of the detector

The channel chosen for this study is $B^0 \to D^{*-}\pi^+$ where the $D^*$ decays; $D^{*-} \to \overline{D}^0\pi^-$ then to $\overline{D}^0 \to K^+\pi^-$. This channel will be able to be fully reconstructed with a small background hence giving a clear signal for beauty.

Figure 20 is an example of how a direct beauty meson would look in the MVD using the new event display. This is one of the events chosen in the decay channel, and has been passed through the detector simulation of the detector after the upgrade.

| Decay Channel | PDG Branching Ratio |
|---|---|
| $B^0 \to D^{*-}\pi^+$ | $(2.76 \pm 0.21) \times 10^{-3}$ % |
| $D^{*-} \to \overline{D}^0\pi^-$ | $(67.7 \pm 0.5)$ % |
| $\overline{D}^0(bar) \to K^+\pi^-$ | $(3.83 \pm 0.09)$ % |

Table 4: $B^0 \to D^{*-}\pi^+$, $D^{*-} \to \overline{D}^0\pi^-$, $\overline{D}^0(bar) \to K^+\pi^-$, PDG branching ratio values

The Pythia branching ratios were tuned accordingly[2] and Monte Carlo generated. This was then put through a simulation of the Zeus detector response known as "funnel". Funnel is at the moment in its upgrade development stage due to all of the new components being added into it.

From Table 4 it can be calculated that one event in 10000 $B^0$'s will follow the decay path that is of interest here. Monte Carlo was used as in the DIS study to see how many events would be found. 225 million events were generated to pick out 1000 events in the desired decay channel in an unbiased manner. For the funneled Monte Carlo, 20000 events were generated but the samples branching rations were modified so that the $B^0$ always decayed to the decay channel understudy to minimize CPU usage. From the sample of direct photoproduction Monte Carlo with a cross section of $7.227\mu b$ the total number of events for 100 $nb^{-1}$ of luminosity was 7227 events. With the acceptance factor included there is expected to 32 ± 5 events. This will be increased by the number of $B^O$ to be found in the resolved channel, as well as expecting the observed cross sections be a factor two to three above the predictions as found by previous studies [13, 14]. This therefore looks promising for an analysis, with an initial small sample.

### 5.2 $D^*$ Tagging with the GTT

One of the ways $B^0$ will be identified will be via $D^*$. The GTT will play a role in tagging these on line. What has been looked at is how efficient GTT algorithm in CTD-SLT mode and in CTD+MVD mode, with respect to the offline $D^*$ reconstruction.

Figure 21 shows the reconstruction of the $D^*$ peak by VCTRACK [16] with is the standard offline tracking package. Figure 22 and Fig. 23 show the fit to the $D^*$ peaks found by the GTT in CTD mode and in CTD+MVD mode with funneled $B^0$ Monte Carlo through the newly released funnel test version including the MVD. Therefore this contains realistic geometry and physical effects.

The $D^*$'s were found in the case of VCTRACK using a standard reconstruction routine [17]. In the case of the GTT the combinatorial method was used, combining tracks to reconstruct the mass of the $D^*$ and selecting the correct charge tracks for the $D^*$ candidate. A simple Gaussian fit to each figure is used to extract the number of $D^*$ candidates. The cuts used to select the $D^*$ are $P_T$ $(K, \pi)$ $>$ 0.45 GeV, 1.8 $<$ $m(D^0)$ $<$ 1.92 GeV, then the mass of the slow pion $P_T(\pi_s)$ (so named due to its low energy) is combined. The $D^*$

[2] the default branching ratios differ

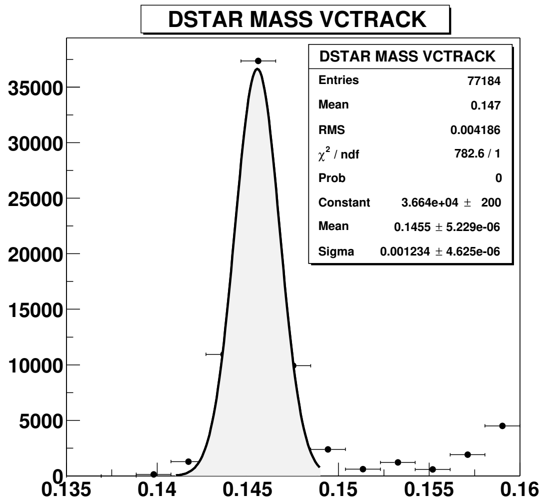


Figure 21: $D^*$ mass using vctrack offline reconstruction

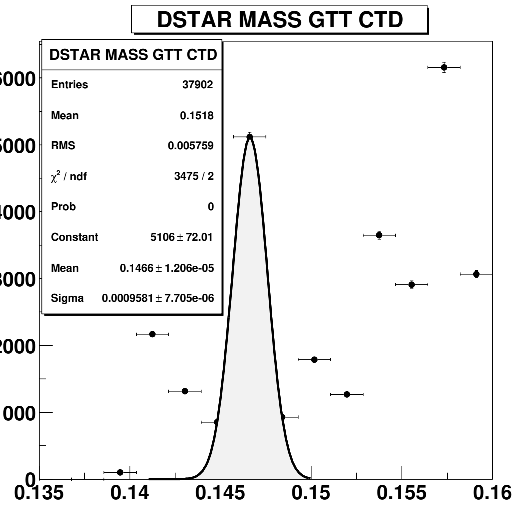


Figure 22: $D^*$ mass using the GTT algorithm in CTD-ONLY mode reconstruction

candidate then has a cut of $P_T(D^*) > 3$ GeV and $|\eta(D^*)| < 1.5$ for the case of the CTD+MVD a cut of $|\eta(D^*)| < 1.0$ was used to make sure that the kinematic region was within the acceptance region of the MVD.

The Gaussian fits are effected by different regimes, in Fig. 23 the lower $D^*$ mass region is affected by the CTD-ONLY part of algorithm therefore a double Gaussian would have been more realistic. There is also the problem that the GTT wrongly assumes a vertex (0,0,0) cm which will make an improvement when changed to the correct vertex (1.75,0,0) cm. The number of events is extracted in a naive way here; Normalizing the wrong charge background to the signal then subtracting the background, or going through the fitting procedure with a background function added to extract the number of $D^*$ candidates would have given a more stable result. This will be done, time was a limiting factor in this case.

In the case of the CTD-ONLY mode the resolution is misleading and this should be combined with another to understand the CTD acceptance. Correction factors calculated show that for the GTT in stand alone mode within an eta range of $|\eta| < 1.0$ approximately 68% of $D^*$'s are found with VCTRACK being the benchmark to which all are compared. In the region $|\eta| < 1.5$ for the CTD-ONLY the factor is 26% and finally in CTD+MVD mode in the region $|\eta| < 1.0$ the factor is 90% efficient. Note, these are rough $1st$ estimates.

This clearly shows that the GTT has the potential to tag $D^*$ decays with a resolution better then that of the current VCTRACK without MVD information. This would mean online that there could be an extra requirement in $D^*$ triggers to

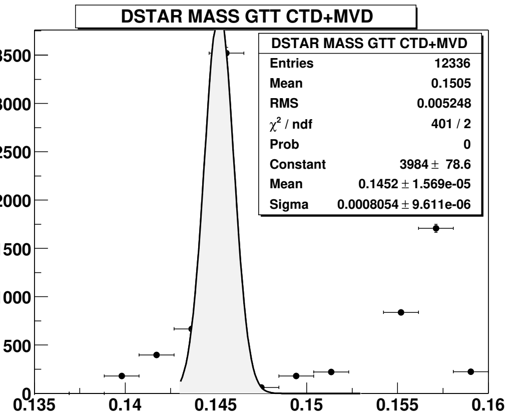


Figure 23: $D^*$ mass using the GTT algorithm in CTD+MVD mode reconstruction

require an "or" of the GTT in either CTD only mode or CTD+MVD mode to keep events such as these which maybe lost due to other requirements not being satisfied in the triggers. This gives a first glimpse at the power of the MVD for heavy flavour studies.

# 6 Conclusions

The work I have carried out has been diverse, which to me describes Zeus. The CFLTP is in good shape and the likelihood of the first direct measurement of beauty production at HERA with the new MVD is promising. This year has been very exciting in many ways, I have enjoyed the time I have spend on Zeus and hope to continue to do so.

## 7 Acknowledgments

I would like to thank thoughs who have helped me over that past year. In particular Antonio Pellegrino and Danny Krakauer for being excellent teachers, whilst being patient with me and great fun to work with in teaching me the way of the CFLTP, Richard Hall-Wilton for teaching me all about Zeus and helping me in all that I do, Sergei Chekanov for always answering my questions, helping me, and putting up with me in the office, and Mark Sutton for solving coding problems when I get stuck.

## References

[1] K.Tokushuku *GFLT Design Document I - interface to component - ( version 5.1 )*, Zeus Note **88-98**

[2] W.H.Smith, M.Jaworski, J.Lackey, P.Robl *Zeus Calorimeter First Level Trigger*, Zeus Note **89-085**

[3] W.H.Smith, I.Ali, B.Behrens, C.Fordham, C.Foudas, A.Goussiou, M.Jaworski, T.Kinnel, J.Lackey, P.Robl, S.Silverstein, J.W.Dawson, D.A.Krakauer, R.L.Talaga, J.L.Schlereth *Zeus Calorimeter First Level Trigger*, Nuclear Instruments and Methods **A 355**

[4] W.Badgett *Programming, Testing and Debugging CFLT Adder Cards*, Zeus Note **96-058**

[5] R.L.Talaga, J.W.Dawson *Conceptual Design of the Calorimeter First-Level Trigger Processor*, Zeus Note **89-086**

[6] A.Caldwell, G.Feild, A.Freidhof, L.Hervás, J.N.Lim, B.Y.Oh, S.Ritz, T.Tsurugai, R.Yoshida *The time calibration of the ZEUS Calorimater*, Zeus Note **93-021**

[7] J.Loizides, A.Polini, A.Savin *The CAL and CFLT timing calibration*, Zeus Note **02-010**

[8] J.R.Goncalo, K.Long *A minimum bias vertex distribution for the* 1998/99 $e^-p$ *data*, Zeus Note **00-027**

[9] M.Sutton, C.Youngman *The Global Tracking Trigger System and Architecture*, Zeus Note **99-074**

[10] R.Hall-Wilton, M.R.Sutton, B.J.West *The CTD-BMVD version 3.3 Global Tracking Trigger Algorithm and Performance*, Zeus Note **01-039**

[11] B.West *Charm and the Virtual Photon at HERA and Global Tracking Trigger for ZEUS*

[12] T.Sjöstrand, L.Lönnblad *Pythia 6.2 Physics and Manual* **hep-ph/0108264**

[13] ZEUS Collaboration; J.Breitweg et al. *Measurement of open beauty production in photoproduction at HERA* **DESY 00-166**

[14] H1 Collaboration; C.Adloff et al. *Measurement of Open Beauty Production at HERA* **hep-ex/9909029**

[15] G.Ingelman, J.Rathsman, G.Schuler *AROMA 2.2 - A Monte Carlo Generator for Heavy Flavour Events in ep Collisions* **DESY 96 058**

[16] G.F.Hartner, Y.Iga, J.B.Lane, N.A.McCubbin *VCTRAK (3.06/11): Offline Output Information* **95-004**

[17] L.Gladilin *http://www-zeus.desy.de/~gladilin/ZEUS_ONLY/zcharm/zcharm.html*

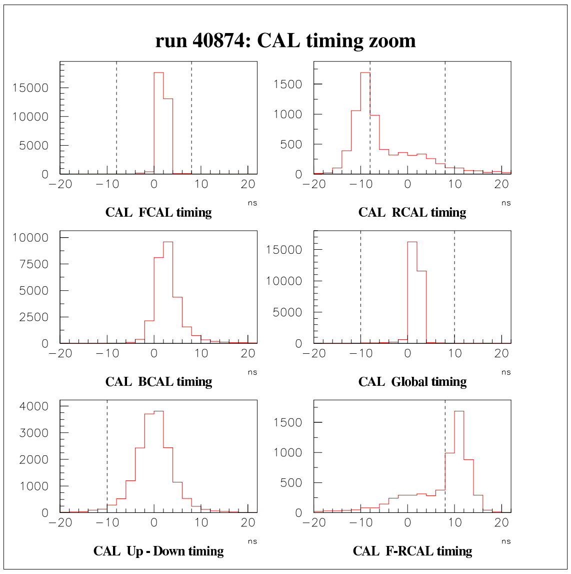


Figure 24: Timing Distributions from The Global Second Level Presenter for a calibrated Proton Timing

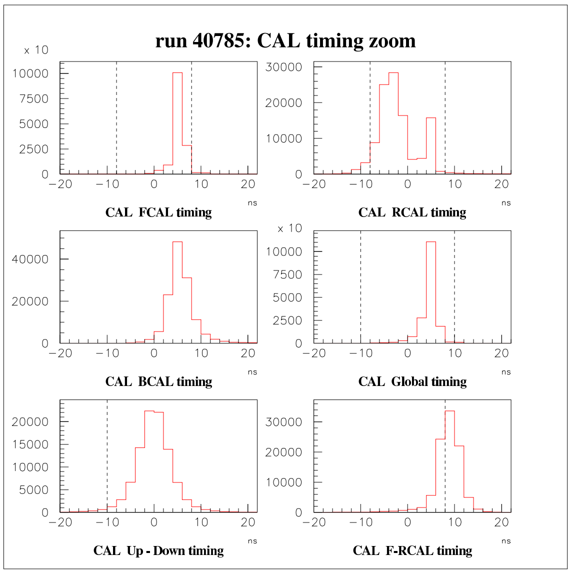


Figure 25: Timing Distributions from The Global Second Level Presenter un-calibrated Proton Timing